A&A 508, 963–969 (2009)
DOI: 10.1051/0004-6361/200912526

Astronomy & Astrophysics

On the origin of reverse polarity patches found by *Hinode* in sunspot penumbrae

J. Sánchez Almeida[1,2] and K. Ichimoto[3]

[1] Instituto de Astrofísica de Canarias, 38205 La Laguna, Tenerife, Spain
e-mail: jos@iac.es
[2] Departamento de Astrofísica, Universidad de La Laguna, Tenerife, Spain
[3] Kwasan and Hida Observatories, Kyoto University, Yamashina, Kyoto 607-8471, Japan
e-mail: ichimoto@kwasan.kyoto-u.ac.jp

Received 19 May 2009 / Accepted 17 September 2009

ABSTRACT

Context. The topology of penumbral magnetic fields is poorly known. The satellite *Hinode* has recently revealed penumbral structures of a magnetic polarity that is opposite to the main sunspot polarity. They may be direct confirmation that magnetic field lines and mass flows return to the solar interior throughout the penumbra, a configuration previously inferred from interpretation of observed Stokes profile asymmetries.
Aims. We try to point out the relationship between the reverse polarity features found by *Hinode*, and the model Micro-Structured Magnetic Atmospheres (MISMAs) proposed for sunspots.
Methods. The work is based on synthesis and inversion of sunspot Stokes profiles.
Results. Existing model MISMAs produce strongly redshifted reverse polarity structures as found by *Hinode*. Ad hoc model MISMAs also explain the asymmetric Stokes profiles observed by *Hinode*. The same modeling may be consistent with magnetograms of dark cored penumbral filaments if the dark cores are associated with the reverse polarity. This hypothetical relationship can only be identified in the far red wings of the spectral lines.
Conclusions. The reverse polarity patches may result from aligned magnetic field lines and mass flows that bend over and return to the solar interior throughout the penumbra.

Key words. Sun: magnetic fields – Sun: photosphere – sunspots

1. Rationale

Sunspots have always been benchmarks for testing our understanding of magneto-convection. It has long been known that magnetic forces impede the free plasma motions, thus reducing the efficiency of convection (Biermann 1941; Cowling 1953). However, convection occurs in sunspots independently of the intense field strength and the high conductivity of the photospheric plasma. The main problem is identifying the mode of convection, i.e., how magnetic fields and plasma flows adjust one another to allow transporting the energy that balances the radiation losses. This long-lasting problem is far from been settled, and it is particularly severe in the penumbrae of sunspots with predominantly horizontal magnetic fields and mass flows (for reviews see, e.g., Solanki 2003; Thomas & Weiss 2004; Schlichenmaier 2009; Sánchez Almeida 2009; Thomas 2009). From an observational point of view, the problem lies in the small physical scales on which the convective transport is organized. Even with the highest spatial resolutions yet achieved, we cannot follow the rise, cooling, and subsequent submergence of plasma blobs. The topology of the magnetic field lines and flows must be inferred indirectly. The present paper is devoted to analyzing and interpreting a recent observation that may be central to constraining the topology of the magnetic fields in penumbrae.

Ichimoto et al. (2007) report the presence of a strongly redshifted magnetic component in the penumbrae of sunspots with a polarity opposite to the main sunspot polarity. This component shows up throughout the penumbra, a property used to argue that the redshift must be due to vertical velocities. The observations were carried out with the satellite *Hinode* (Kosugi et al. 2007), which yields a spatial resolution of 0.″32 at the wavelength of operation (≃6302 Å; Tsuneta et al. 2008). The finding of Ichimoto et al. seems to be at variance with the magnetograms taken by Langhans et al. (2005, 2007) with the Swedish Solar Tower (SST, Scharmer et al. 2002), which do not show magnetic fields of reverse polarity in penumbrae. This poses a serious problem since SST has twice the spatial resolution of *Hinode* and, therefore, it should be simpler for SST to resolve and detect mixed polarities. SST magnetograms only reveal a decrease of the magnetograph signals coinciding with the dark cores, i.e., the dark lanes outlined by bright filaments discovered by Scharmer et al. (2002). This work shows how *Hinode* and SST observations can be naturally understood within the two-component semi-empirical model penumbra derived by Sánchez Almeida (2005, hearafter SA05), provided that the dark cores are associated with the reverse polarity.

SA05 works out the model micro-structured magnetic atmospheres (MISMAs[1]) required to quantitatively reproduce the

[1] The acronym was coined by Sánchez Almeida et al. (1996) to describe magnetic atmospheres with optically-thin substructure, which naturally produce asymmetric spectral lines.

asymmetries of the Stokes profiles[2] observed in a large sunspot. Other inversion techniques have succeeded in reproducing the observed line shapes (e.g., Sánchez Almeida & Lites 1992; Westendorp Plaza et al. 2001; Mathew et al. 2003), but there is something unique to the MISMA inversion, namely, the model demands two opposite polarities. This unexpected result has been often criticized as being unreal (e.g., Langhans 2006; Bellot Rubio 2009), although it is the ingredient that naturally explains *Hinode* reversals. The MISMA model sunspot includes two magnetic components. The major component contains most of the mass of each resolution element and has the polarity of the sunspot. It is generally combined with a minor component of opposite polarity and large velocity. In typical 1″-resolution observations, the outcoming light is systematically dominated by the major component, and the resulting Stokes profiles have rather regular shapes. An exception occurs in the so-called *apparent neutral line*, where the Stokes V profiles show a characteristic shape with three or more lobes termed the *cross-over effect* (see Sánchez Almeida & Lites 1992, and references therein). At the neutral line the mean magnetic field vector is perpendicular to the line-of-sight, and the contribution of the major component almost disappears in Stokes V due to projection effects. The cancellation of the two components is expected to be less effective when improving the spatial resolution, leading to the appearance of cross-over profiles. Actually, *Hinode* often detects cross-over Stokes V profiles, and they show up at precisely the location of the reverse polarities (Fig. 5 in Ichimoto et al. 2007, and also Sect. 3). The observed cross-over profiles have two polarities: the main sunspot polarity close to the line center, and the reverse polarity at the far red wing. Since the reverse polarity patches detected in penumbrae by *Hinode* produce cross-over profiles, they seem to correspond to structures where the polarity is not well defined, with positive and negative polarities coexisting in each pixel.

The paper is structured as follows. Section 2 shows how the model MISMAs from SA05 qualitatively reproduce both *Hinode* and SST observations. We develop a simple model penumbral filament to demonstrate that it can reproduce all the essential features of the observed ones. The same agreement is found when the model MISMAs are inferred by fitting *Hinode* Stokes profiles (Sect. 3). The implications of our work in the context of the penumbral magnetic field topology and the Evershed effect are discussed in Sect. 4, where we also put forward a specific test that could confirm or falsify our interpretation. Empirical and theoretical difficulties of the association bewteen dark cores and reverse polarities are also discussed in Sect. 4.

2. Model MISMA for penumbral filaments with dark cores

As described in the introduction, the model MISMAs often require two magnetic components with opposite polarities to reproduce the observed Stokes profiles. The major component has the polarity of the sunspot, and it is combined with a minor component of opposite polarity and large velocities[3]. The emitted light is dominated by the major component, so that the reverse polarity seldom produces an obvious signal in the spatially integrated Stokes profiles. In this scenario, improving the spatial resolution would reduce the spatial smearing, allowing extreme cases to show up. To mimic the effect of improving spatial resolution, several randomly chosen model MISMAs in SA05 were modified by increasing the fraction of atmosphere occupied by the minor component. Now the minor component shows up in Stokes V. The behavior that we will describe is common to all the models, but we examine in detail only the example given in Fig. 1. The resulting Stokes I, Q, and V profiles of Fe I λ6302.5 Å are represented as solid lines in Figs. 1a–c, respectively. They correspond to a point in the limb-side penumbra of a sunspot at $\mu = 0.95$ (18° heliocentric angle). Note how Stokes I is redshifted and deformed, and how Stokes V shows the cross-over effect. Consequently, the improvement of spatial resolution with respect to traditional earth-based spectropolarimetric observations naturally explains the abundance of cross-over Stokes V profiles found by *Hinode*. Figures 1a–c also show the case where the major component dominates (the dashed line). The strong asymmetries have disappeared, rendering Stokes V with reasonably antisymmetric shape and the sign of the dominant polarity. We recall that the two sets of Stokes profiles in Figs. 1a–c (the solid lines and the dashed lines) have been produced with exactly the same magnetic field vectors and mass flows (shown in Figs. 1e and f). The atmospheres differ because of the relative importance of major and minor components, and because of a global scaling factor in the temperature stratification. One of them is some 80% cooler than the other. The coolest exhibits asymmetric profiles of low continuum intensity, suitable to mimic dark features (see the Stokes I continua in Fig. 1a).

Interpreting *Hinode* observations in terms of MISMAs also explains the lack of reverse polarity in SST magnetograms. In reverse polarity regions, Stokes V shows the cross-over effect (Fig. 5 in Ichimoto et al. 2007, and the solid line in Fig. 1c), i.e., it presents two polarities depending on the sampled wavelength. It has the main sunspot polarity near line center, whereas the polarity is reversed in the far red wing. SST magnetograms are taken at line center (±50 mÅ), which explains why the reverse polarity does not show up. However, a significant reduction in the Stokes V signal occurs. Such reduction naturally explains the observed weakening of magnetic signals in dark cores (Langhans et al. 2005, 2007, and Sect. 1), provided that the dark cores are associated with an enhancement of the opposite polarity, i.e., if the dark cores produce cross-over profiles. In order to illustrate the argument, we construct images, magnetograms, and dopplergrams of a (naïve) model dark-cored filament. It is formed by a uniform 100 km wide dark strip, which represents the dark core, bounded by two bright strips of the same width, which represent the bright sides. The Stokes profiles of the dark core have been taken as the solid lines in Figs. 1a and c, whereas the bright sides are modeled as the dashed lines in the same figures. The color filters employed by Langhans et al. (2005, 2007) are approximated by Gaussian functions of 80 mÅ *FWHM*, shifted ±50 mÅ from the line center (see the dotted lines in Fig. 1a). The magnetogram signals are computed from the profiles as

$$M = -\frac{\Delta\lambda}{|\Delta\lambda|}\frac{\int V(\lambda) f(\lambda-\Delta\lambda)\,\mathrm{d}\lambda}{\int I(\lambda) f(\lambda-\Delta\lambda)\,\mathrm{d}\lambda}, \quad (1)$$

[2] As usual, the Stokes parameters are used to characterize the polarization: I represents the intensity, Q and U the two independent types of linear polarization, and V the circular polarization. The Stokes profiles are graphs of I, Q, U and V versus wavelength for a particular spectral line. They follow well defined symmetries when the atmosphere has constant magnetic field and velocity (see, e.g., Landi Degl'Innocenti 1992).

[3] Here and throughout, *minor* and *major* refer to the two components in the model sunspot by SA05. When applied to the components in the model atmospheres developed in this paper, it only implies that their magnetic and velocity properties are similar to the minor and major components in SA05.

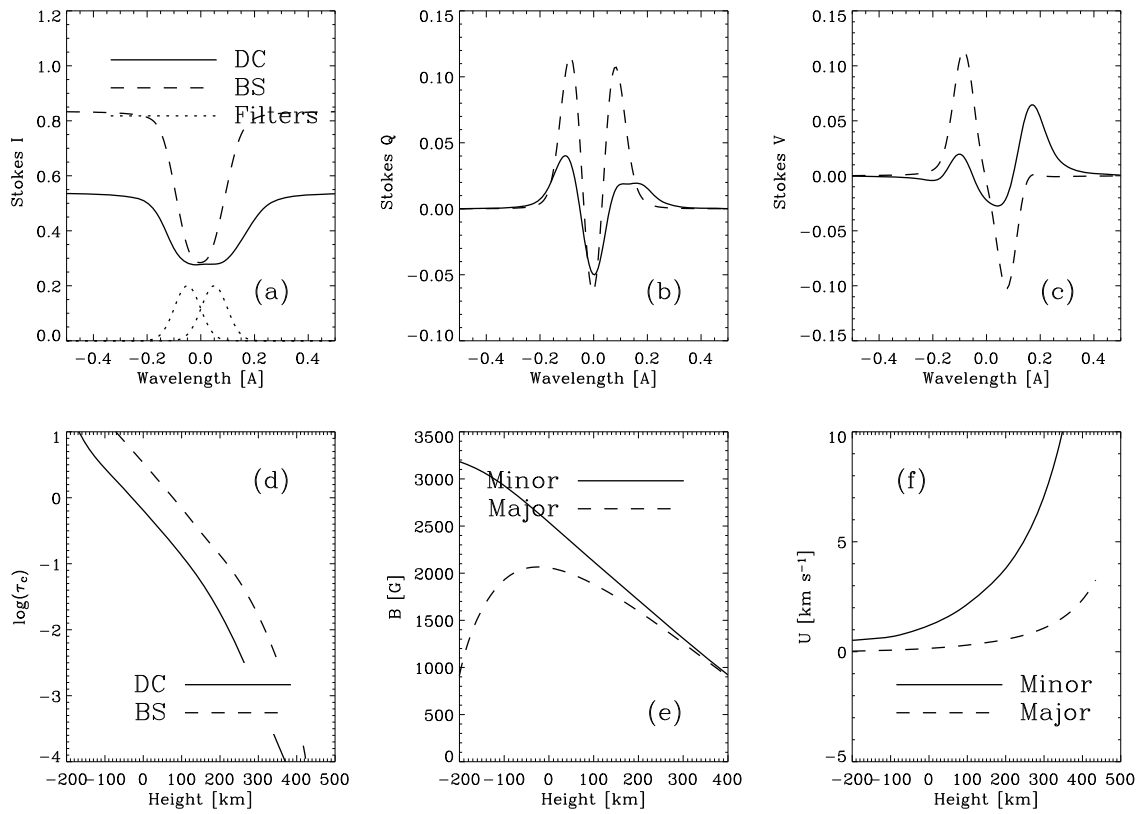

Fig. 1. **a)** Stokes I profiles in one of the representative model MISMAs in SA05, which has been slightly modified to represent a dark core (the solid line), and its bright sides (the dashed line). They are normalized to the quiet Sun continuum intensity. **b)** Stokes Q profiles. **c)** Stokes V profiles. **d)** Continuum optical depth τ_c versus height in the atmosphere for the dark core and the bright sides, as indicated in the inset. **e)** Magnetic field strength versus height for the two magnetic components of the model MISMAs. They are identical for the dark core and the bright sides. **f)** Velocities along the magnetic field lines for the two magnetic components of the model MISMAs. They are identical for the dark core and the bright sides.

where the wavelength λ refers to the central wavelength of the line, $f(\lambda)$ represents the transmission curve of the filter centered at $\lambda = 0$, and $\Delta\lambda = -50$ mÅ. Similarly, the Doppler signals are given by

$$D = \frac{\Delta\lambda}{|\Delta\lambda|} \frac{\int I(\lambda)\,[f(\lambda+\Delta\lambda) - f(\lambda-\Delta\lambda)]\,\mathrm{d}\lambda}{\int I(\lambda)\,[f(\lambda+\Delta\lambda) + f(\lambda-\Delta\lambda)]\,\mathrm{d}\lambda}, \quad (2)$$

but here we employ the Stokes I profile of the non-magnetic line used by Langhans et al. (2007; i.e., Fe I λ5576 Å). When $\Delta\lambda < 0$, the signs of M and D ensure that $M > 0$ for the main polarity of the sunspot, and $D > 0$ for redshifted profiles. The continuum intensity has been taken as I at −0.4 Å from the line center. The continuum image of this model filament is shown in Fig. 2, with the dark core and the bright sides marked as DC and BS, respectively. The dopplergram and the magnetogram are also included in the same figure. The dark background in all images indicates the level corresponding to no signal. In agreement with the observations of Langhans et al., the filament shows redshifts ($D > 0$), which are enhanced in the dark core. In agreement with Langhans et al., the filament shows the main polarity of the sunspot ($M > 0$), the signal being strongly reduced in the dark core. Figure 2, bottom, includes the magnetogram to be observed at the far red wing ($\Delta\lambda = 200$ mÅ). The dark core now shows the reverse polarity ($M < 0$), whereas the bright sides still maintain the main polarity with an extremely weak signal. This specific prediction of the modeling is amenable to direct observational test (see Sect. 4).

Two additional remarks about our modeling are in order. First, the magnetogram signal in the dark core is much weaker than in the bright sides, despite the (average) magnetic field strength being larger in the core (see Fig. 1e, keeping in mind that the minor component dominates). Second, the model dark core is depressed in height with respect to the bright sides. Figure 1d shows the continuum optical depth τ_c as a function of the height in the atmosphere. When the two atmospheres are in lateral pressure balance, the layer $\tau_c = 1$ of the dark core is shifted by some 100 km downward with respect to the same layer in the bright sides. The depression of the observed layers in the dark core is produced by two conspiring effects: the decrease in density associated with the increase in magnetic pressure (e.g., Spruit 1976), and the decrease in opacity associated with the reduction in temperature (e.g., Stix 1991). We mention the association of our dark cores with enhanced field strength and with geometrical depression because these properties contrast with some popular models of penumbral magneto-convection (e.g., Scharmer & Spruit 2006; Rempel et al. 2009). We note, however, that the association between field strength, brightness, and geometrical height is far from being established. Not all models predict dark features coinciding with weaker fields. The siphon flow model of the Evershed effect has enhanced field strengths in the downflowing leg (e.g., Schlichenmaier 2002). The plasma has already cooled when reaching this footpoint and, so, one expects to find downflows associated with stronger fields and colder plasmas. As far as the elevation of the dark cores is concerned, a solid observational result disfavors it.

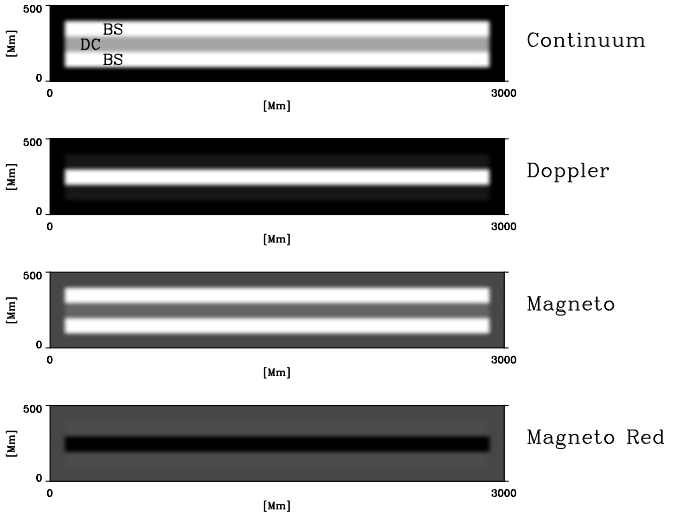

Fig. 2. Schematic modeling of SST observations of penumbral filaments by Langhans et al. (2005, 2007). A dark core (DC) surrounded by two bright sides (BS) is located in the limb-side penumbra of a sunspot at $\mu = 0.95$ (i.e., 18° heliocentric angle). The three top images show a continuum image, a dopplergram, and a magnetogram, as labelled. The convention is such that both the sunspot main polarity and a redshift produce positive signals. The dark background in all images has been included for reference and corresponds to a signal that equals zero. The fourth image (`Magneto Red`) corresponds to a magnetogram in the far red wing of Fe I λ6302.5 Å, which exhibits a dark core with a polarity opposite to the sunspot main polarity. The continuum image and the dopplergram have been scaled from zero (black) to maximum (white). The scaling of the two magnetograms is the same, so that their signals can be compared directly.

Schmidt & Fritz (2004) found that the limb-side penumbra and the center-side penumbra are darker than the rest. They interpret this observation as being an effect of the depression of the dark penumbral filaments, which are obscured by the bright ones when observed sideways. Obviously, this is an average result, but it strongly suggests that if dark cores are common, then they must be depressed with respect to the bright sides. We show here how the reduced magnetograph signals observed in dark cores can be produced even if their field strength is enhanced.

3. Reproducing *Hinode* Stokes profiles

We have gone a step further, and the exercise in the previous section has been repeated using model MISMAs derived directly from *Hinode*/SP data. We use a small set of seven Stokes profiles selected as extreme cases among the entire range of redshifted and blueshifted profiles. They were observed in a simple, positive-polarity sunspot (NOAA10944) when the target was almost at the solar disk center (heliocentric angle 1°.1), so that the line-of-sight direction and the vertical direction coincide for most purposes. The observation is described in Ichimoto et al. (2008), to which we refer for images, a logbook, and further details. Our data correspond to those taken at 18:25 UT on February 28th, 2007. Normal scan maps were obtained with the Spectro-Polarimeter (SP) of the Solar Optical Telescope (SOT; Tsuneta et al. 2008; Suematsu et al. 2008) aboard Hinode (Kosugi et al. 2007). The SP took full Stokes profiles of Fe I λ6301.5 Å and Fe I λ6302.5 Å with 0.1% photometric accuracy, and a spatial sampling of 0″.16.

The MISMA inversion procedure described in Sánchez Almeida (1997) provides reliable fits to the data in all cases. Two examples are shown in Figs. 3 and 5. The dotted lines in Fig. 3 correspond to one representative reverse polarity site. The fit, shown as solid lines, yields the model atmosphere represented in Fig. 4. The inversions were carried out as described in SA05, which we refer to for details. The only significant difference was the setting up of the absolute wavelength scale, which we zeroed from the average intensity profile in a quiet Sun region far from the sunspot. The wavelength of the core of Fe I λ6302.5 Å is assumed to correspond to a global velocity equals to the convective blueshift of the line measured by Dravins et al. (1981). Figures 5 and 6 are similar to Figs. 3 and 4, except that they represent a point with a clear blueshift. The model atmospheres are similar, except that the minor component does not have reverse polarity for these strongly blueshifted profiles. The four panels in Figs. 4 and 6 represent the stratification with height in the atmosphere of (a) magnetic field strength; (b) density; (c) fraction of atmosphere occupied by each component; and (d) velocity along magnetic field lines. The minor component occupies a significant fraction of the atmosphere (some 40% in the examples in the figures), and it has low density and high field strength. Field strengths and densities are similar to those found in SA05, although the fraction of atmosphere occupied by the minor component is significantly higher (almost twice the typical 20% in SA05). This was expected since for inversion we selected pixels with particularly large asymmetries, where the contribution of the minor component must exceed the average to cause a significant impact on the Stokes profiles.

We have repeated the exercise of producing the synthetic magnetograms and dopplergrams in Fig. 2, but using the model MISMAs in Figs. 4 and 6. Specifically, we use the profiles in the blueshifted region to represent the bright sides, and the redshifted profiles for the dark core. The result is shown in Fig. 7. The main features of Fig. 2 remain: (1) the bright filament has a dark core; (2) the line-center magnetogram has a weakening coinciding with the dark core; (3) bright sides are blueshifted with respect to the dark cores; and (4) the far red wing magnetogram shows opposite polarity coinciding with the dark core. Note that features 1−3 are in agreement with SST observations.

A clarification may be appropriate. The association between the Stokes profiles in Fig. 3 and dark cores, and the profiles in Fig. 5 and bright sides is a mere working hypothesis. *Hinode* spectra are hardly able to resolve bright sides and dark cores and, therefore, the used profiles do not correspond to identifiable bright sides and dark cores. We have selected them because they illustrate the properties expected for bright sides and dark cores according to the modeling in Sect. 2. Even with limited resolution, just by chance, some pixels may have enhanced contribution of bright sides and dark cores.

4. Discusion

The model MISMAs by SA05 predict and produce strongly redshifted reverse polarity structures similar to those found by *Hinode* in penumbrae (Sect. 1). In addition to pointing out this agreement (Sect. 2), we have applied the kind of modeling employed by SA05 to quantitatively reproduce some representative very asymmetric Stokes profiles observed by *Hinode* (Sect. 3). In order to fit the Stokes V profiles with three lobes observed in reverse polarity regions (cross-over profiles), the model MISMAs have two components of opposite polarity in each resolution element. The minor component holds the reverse polarity and always transports strong magnetic-field-aligned flows. High spatial resolution SST magnetograph observations of penumbra do

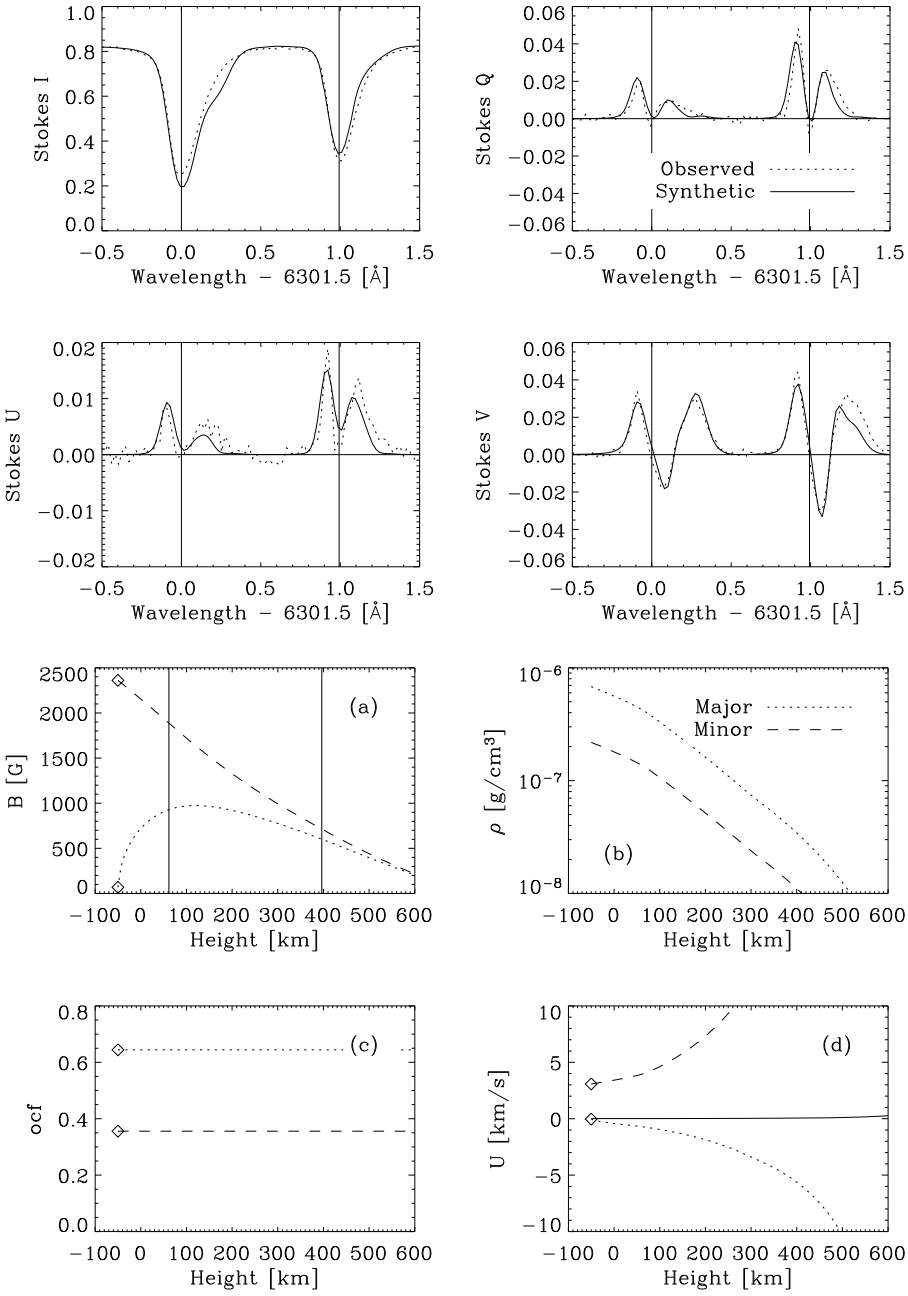

Fig. 3. Set of Stokes profiles of Fe I λ6301.5 Å and Fe I λ6302.5 Å observed by *Hinode* in one of the reverse polarity regions (the dotted lines). (The ordinate axis labels identify the Stokes parameter.) Note how Stokes V shows the cross-over effect (i.e., three lobes rather than two). The solid lines correspond to a MISMA inversion of this set of profiles, and it renders the model atmosphere shown in Fig. 4. Wavelengths are referred to the laboratory wavelength of Fe I λ6301.5 Å. The vertical solid lines indicate the laboratory wavelengths of Fe I λ6301.5 Å and Fe I λ6302.5 Å.

Fig. 4. Model MISMA for one of the typical cross-over profiles. It has been derived from inversion of the profiles shown in Fig. 3, the dotted lines. **a)** Stratification of magnetic field strength. As the inset in **b)** indicates, the minor and the major components can be identified by the type of line. **b)** Stratification of density. **c)** Fraction of the atmosphere occupied by the two components. **d)** Stratification of velocity along magnetic field lines. Note that in order to obtain the Doppler shifts, the velocity U has to be corrected for the inclination of the magnetic field. As the minor and major components have opposite polarities, both yield redshifts. (The magnetic field inclinations of the major and minor components are 74° and 144°, respectively, so that the major component has positive polarity whereas the minor component has negative polarity.) The symbols correspond to the quantities used as free parameters during fitting, which set the full stratification of the atmosphere via MHD constraints (Sánchez Almeida 1997).

not show reverse polarities. They just indicate a weakening of the Stokes V signal that coincides with the dark cores (Langhans et al. 2005, 2007). The presence of reverse polarities and the absence of their signals in SST magnetograms can be explained if the dark cores are associated with reverse polarity Stokes V profiles. Such an association has not been revealed so far because the existing magnetograms were taken at line core, whereas the reverse polarity only shows up in the far red wing of the spectral lines. By tuning the bandpass of SST magnetograms to the appropriate wavelength, this specific prediction of our modeling can be tested observationally[4]. The association between cross-over Stokes V profiles and dark cores is still mere conjecture. However, we note an independent Hinode/SP observation that also suggests this association. Bellot Rubio et al. (2007) find and discuss the case of a limb-side penumbra dark core that clearly shows cross-over Stokes V profiles (see their Fig. 2). As we argue in the introduction, Hinode/SP spatial resolution does not suffice to properly resolve dark cores, but the observation by Bellot Rubio et al. is encouraging. It indicates that the dark cores are associated with several magnetic field inclinations in the resolution element.

The magnetic fields that we use in Sect. 3 to reproduce the observed asymmetries are rather horizontal. However, the flows along field lines are so intense (in excess of 10 km s^{-1} in the minor component; see the botton right panels in Figs. 4 and 6) that the vertical component of the velocities are of the order of a few km s^{-1}. Order of magnitude estimates show that 1 km s^{-1} suffices to explain the transport of energy by convection in penumbrae (e.g., Spruit 1987; Stein & Nordlund 1998; Sánchez Almeida 2009). For the transport to be effective, vertical velocities of such magnitude should be present everywhere.

[4] Even if our prediction turns out to be incorrect, the disagreement between *Hinode* and SST magnetograms is a serious problem that urges solution.

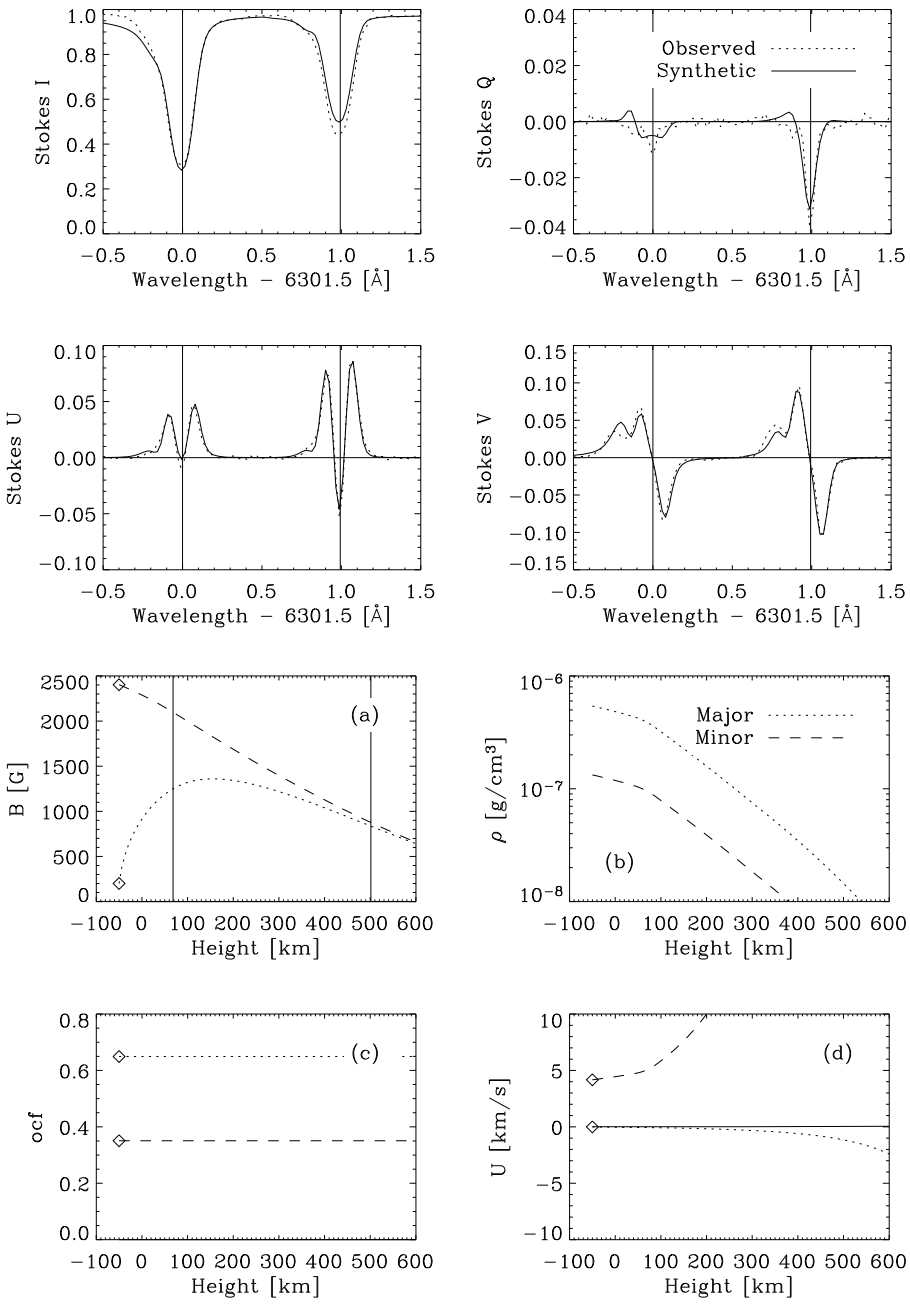

Fig. 5. Same as Fig. 3 but for one of the strongly blueshifted regions. In this case the solid lines correspond to the model atmosphere in Fig. 6.

Fig. 6. Model MISMA reproducing one of the typical blueshifted profiles (the dotted lines in Fig. 5). See caption of Fig. 4 for a description of the various plots. The inclinations of the major and minor components are 66° and 39°, respectively, so that both components have positive polarity. After correcting U for the magnetic field inclination, the velocity of the minor component along a vertical line-of-sight corresponds to blueshifts. The difference from Fig. 4 is due to the flip of the minor component polarity, which is negative in Fig. 4 and positive here.

It is still unclear whether such large velocities are common enough to be responsible for the required convective transport, and this possibility must be studied in detail.

Hinode observations show that the reversals prefer the outer penumbra, whereas asymmetric blueshifted profiles (such as those in Fig. 5) cluster toward the inner penumbra (Ichimoto et al. 2007). One might suspect that this would compromise our interpretation, because dark cores tend to appear in the inner penumbra. However, we caution against over-simplified interpretations of *Hinode* spectra. *Hinode*/SP does not resolve individual dark cores and bright sides, but spatially integrates them. If the bright sides dominate, then the resulting Stokes V profiles would exhibit properties of the bright sides, even if the pixel contains a dark core. Actually, blueshifted profiles seem to be associated with bright continuum features, supporting that the bright sides dominate these points. As one moves toward the outer penumbra, the magnetic field of the bright sides becomes more horizontal, reducing the Stokes V signals and causing the dark core polarization to show up. In agreement with this conjecture, the reverse polarity patches seem to coincide with dark lanes (Ichimoto et al. 2007).

Insufficient resolution may also explain the different morphological appearance of the *Hinode* polarity reversals and the SST dark cores. Dark cores are elongated features, but the locations of downflows described by Ichimoto et al. (2007) are far more point-like features. Cross-over Stokes V signals critically depend on the orientation of the magnetic fields with respect to the line-of-sight. Small modifications of the magnetic field geometry would make the reverse polarity to become unobservable, overwhelmed by the Stokes V signals of the main sunspot polarity. The reverse polarity shows up only when a number of conditions are met, but this need to satisfy several subtle tradeoffs makes the presence of identifiable reverse polarities rare, therefore, they tend to be spatially scattered, discontinuous, and so point-like. In contrast, these delicate balances do not affect the intensity and, therefore, unpolarized light SST images tend

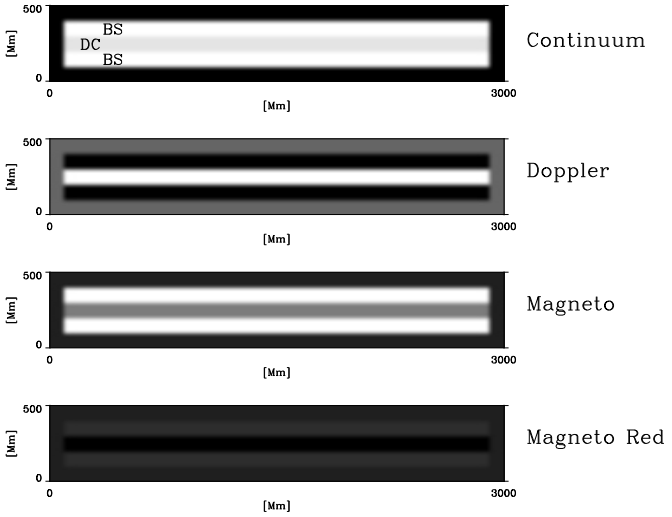

Fig. 7. Set of synthetic images, dopplergrams and magnetograms equivalent to Fig. 2, but using the model MISMAs directly derived from *Hinode* spectra to represent the dark core and its bright sides. The main features are similar to those of Fig. 2.

to show more continuous structures with the filamentary appearance characteristic of penumbrae.

A final important comment is in order. Stokes V profiles such as those in Figs. 3 and 5 have net circular polarization (NCP), i.e., the wavelength integral of the Stokes V profile differs from zero. NCP can *only* be produced by variations of the magnetic field and velocity *along* the line-of-sight, which is well known from the early works to explain the broad-band circular polarization in sunspots by Illing et al. (1975) and Auer & Heasley (1978) (see, e.g., Sánchez Almeida & Lites 1992, and references therein). This implies that strongly asymmetric Stokes V profiles showing NCP will always be present in sunspots, regardless of the spatial resolution of the observation *across* the line-of-sight. Even if the resolution of our telescope could be improved to infinity, we would never be able to separate the penumbrae into pixels where the magnetic field is uniform. In other words, resolving the fine-scale structure of the penumbral magnetic field is not (only) a question of improving the spatial resolution, but requires an understanding of the line asymmetries. Whether this understanding requires MISMAs or can be accomplished with a smoother magnetic field distribution is still a matter of debate (e.g., SA05, Sect. 5; Langhans 2006).

Acknowledgements. Hinode is a Japanese mission developed and launched by ISAS/JAXA, with NAOJ as domestic partner and NASA and STFC (UK) as international partners. It is operated by these agencies in co-operation with ESA and NSC (Norway). The work has partly been funded by the Spanish Ministry of Science and Technology, project AYA2007-66502, as well as by the EC SOLAIRE Network (MTRN-CT-2006-035484). This work was partly carried out at the NAOJ Hinode Science Center, which is supported by the Grant-in-Aid for Creative Scientific Research, The Basic Study of SpaceWeather Prediction from MEXT, Japan (Head Investigator: K. Shibata), generous donations from Sun Microsystems, and NAOJ internal funding.

References

Auer, L. H., & Heasley, J. N. 1978, A&A, 64, 67
Bellot Rubio, L. R. 2009, in Magnetic Coupling between the Interior and the Atmosphere of the Sun, ed. S. S. Hassan, & R. J. Rutten (Berlin: Springer-Verlag), Astrophys. Space Sci. Proc., in press [arXiv:0903.3619]
Bellot Rubio, L. R., Tsuneta, S., Ichimoto, K., et al. 2007, ApJ, 668, L91
Biermann, L. 1941, Vierteljahrsschr. Astr. Gesellsch., 76, 194
Cowling, T. G. 1953, Solar Electrodynamics, ed. G. P. Kuiper (Chicago: The University of Chicago Press), 532
Dravins, D., Lindegren, L., & Nordlund, A. 1981, A&A, 96, 345
Ichimoto, K., Shine, R. A., Lites, B., et al. 2007, PASJ, 59, 593
Ichimoto, K., Tsuneta, S., Suematsu, Y., et al. 2008, A&A, 481, L9
Illing, R. M. E., Landman, D. A., & Mickey, D. L. 1975, A&A, 41, 183
Kosugi, T., Matsuzaki, K., Sakao, T., et al. 2007, Sol. Phys., 243, 3
Landi Degl'Innocenti, E. 1992, in Solar Observations: Techniques and Interpretation, ed. F. Sánchez, M. Collados, & M. Vázquez (Cambridge: Cambridge University Press), 71
Langhans, K. 2006, in Solar Polarization 4, ed. R. Casini, & B. W. Lites (San Francisco: ASP), ASP Conf. Ser., 358, 3
Langhans, K., Scharmer, G., Kiselman, D., Löfdahl, M., & Berger, T. E. 2005, A&A, 436, 1087
Langhans, K., Scharmer, G. B., Kiselman, D., & Löfdahl, M. G. 2007, A&A, 464, 763
Mathew, S. K., Lagg, A., Solanki, S. K., et al. 2003, A&A, 410, 695
Rempel, M., Schüssler, M., & Knölker, M. 2009, ApJ, 691, 640
Sánchez Almeida, J. 1997, ApJ, 491, 993
Sánchez Almeida, J. 2005, ApJ, 622, 1292
Sánchez Almeida, J. 2009, in Magnetic Coupling between the Interior and the Atmosphere of the Sun, ed. S. S. Hassan, & R. J. Rutten (Berlin: Springer-Verlag), Astrophys. Space Sci. Proc., in press [arXiv:0902.4532]
Sánchez Almeida, J., & Lites, B. W. 1992, ApJ, 398, 359
Sánchez Almeida, J., Landi Degl'Innocenti, E., Martínez Pillet, V., & Lites, B. W. 1996, ApJ, 466, 537
Scharmer, G. B., & Spruit, H. C. 2006, A&A, 460, 605
Scharmer, G. B., Gudiksen, B. V., Kiselman, D., Löfdahl, M. G., & Rouppe van der Voort, L. H. M. 2002, Nature, 420, 151
Schlichenmaier, R. 2002, Astron. Nachr., 323, 303
Schlichenmaier, R. 2009, Space Sci. Rev., 213
Schmidt, W., & Fritz, G. 2004, A&A, 421, 735
Solanki, S. K. 2003, A&ARv, 11, 153
Spruit, H. C. 1976, Sol. Phys., 50, 269
Spruit, H. C. 1987, in The Role of Fine-Scale Magnetic Fields on the Structure of the Solar Atmosphere, ed. E.-H. Schrö ter, M. Váquez, & A. A. Wyller (Cambridge: Cambridge University Press), 199
Stein, R. F. I., & Nordlund, Å. 1998, ApJ, 499, 914
Stix, M. 1991, The Sun (Berlin: Springer-Verlag)
Suematsu, Y., Tsuneta, S., Ichimoto, K., et al. 2008, Sol. Phys., 249, 197
Thomas, J. H. 2009, in Magnetic Coupling between the Interior and the Atmosphere of the Sun, ed. S. S. Hassan, & R. J. Rutten (Berlin: Springer-Verlag), Astrophys. Space Sci. Proc., in press [arXiv:0903.4106]
Thomas, J. H., & Weiss, N. O. 2004, ARA&A, 42, 517
Tsuneta, S., Ichimoto, K., Katsukawa, Y., et al. 2008, Sol. Phys., 249, 167
Westendorp Plaza, C., del Toro Iniesta, J. C., Ruiz Cobo, B., et al. 2001, ApJ, 547, 1130